Metals and Materials International (2021) 27:3695–3708
https://doi.org/10.1007/s12540-020-00868-6

Effect of Ceramic Particulate Addition on Aluminium Based Ex-Situ and In-Situ Formed Metal Matrix Composites

B. Gobalakrishnan[1] · C. Rajaravi[2] · Gobikrishnan Udhayakumar[3] · P. R. Lakshminarayanan[1]

Received: 15 July 2020 / Accepted: 20 August 2020 / Published online: 12 September 2020

Abstract
An attempt was made to synthesis ex-situ formed Al/SiC MMC and in-situ formed Al/TiB_2 MMC using stir casting method with different weight percentage of the ceramic particulates such as 4 wt%, 6 wt% and 8 wt% respectively. Significant improvements of mechanical properties were observed when the addition of reinforcement particulates increased from 2 to 8 wt%. The tensile strength and Rockwell hardness of the ex-situ and in-situ formed composites were conducted as per the ASTM standard E08-16 and ASTM standard E18-15 respectively. The in-situ formed TiB_2 MMC has superior mechanical properties such as 0.2% proof strength, tensile strength and hardness as compared to ex-situ SiC MMC as well as base metal. It is also concluded that the mechanical properties were increased with increase in wt% of reinforcement particles additions. The Optical Microscopy and Scanning Electron Microscopy were used to examine the size and uniformity of reinforcement particles whereas the Energy Dispersive X-ray analysis, X-ray diffractometer and Element Mapping analysis were used to confirm the presence of TiB_2 particles.

Keywords MMCs · Al/SiC · Al/TiB_2 · Stir casting · Microstructure · Mechanical properties

1 Introduction

Many applications require higher strength, hardness, corrosion resistance, wear-resistance and thermal stability, like structural members, IC engine piston and brake shoes need Aluminium with better stiffness, strength with lighter weight. For this reason, castings are made by mixing hard ceramic particles into the molten aluminium matrix and fabricated to form Aluminium based composite materials. [1–5]. Al/SiC MMCs are very stiff at the same time have higher strength to weight ratio and wear resistance. Many aerospace components, sports cars, wear parts, seals and piston rings require lighter materials like Aluminium and magnesium that have higher strength and lighter weight. Aluminium with TiB_2 reinforcement formed in-situ has still higher strength, stiffness and most especially good thermal stability when compared to Al/SiC MMCs. These properties make Al/TiB_2 MMCs very much attractive. Al/TiB_2 MMCs can be competitive to magnesium, presently used material, the melting and fabrication of which is very complicated. Under all these circumstances, Aluminium becomes an attractive choice whether it is cast as such or reinforced with SiC or TiB_2 [6–10].

This paper deals with the effect of reinforcement particles addition on microstructure and mechanical properties such as 0.2% yield strength, Ultimate Tensile Strength (UTS) and hardness of the ex-situ and in-situ formed composites.

2 Experimental Procedure

In this investigation, wrought Aluminium 6061alloy was used as the base metal. The vacuum spectrometer (ARL, model 3460) was employed to estimate the wt% of the individual alloying elements present in the base metal. The spectrums were acquired by igniting sparks at various locations, and their compositions were estimated (Table 1).

✉ B. Gobalakrishnan
bgkrish.mech@gmail.com

[1] Department of Manufacturing Engineering, Annamalai University, Annamalai Nagar, Tamil Nadu 608 002, India

[2] Department of Mechanical Engineering, Vel Tech Multi Tech Dr. Rangarajanm Dr. Sakunthala Engineering College, Chennai, Tamil Nadu 600 062, India

[3] Department of Mechanical Engineering, Sona College of Technology, Salem, Tamil Nadu 636 005, India

Fabrication of ex-situ formed Al/SiC MMCs comprises, Silicon Carbide particles (SiC) with a size of 22 μm with 4 wt%, 6 wt% & 8 wt% were used as reinforcement, Small chips of wrought 6061 Aluminium alloy were loaded in the graphite crucible of the stir casting furnace and started heating. The cut off temperature was fixed at 780 °C. The melt temperature was maintained at 700–750 °C. The current rating was maintained at 20 Amps. SiC powder was pre-heated at 750 °C and maintained with 2 h of soaking in a muffle furnace and then pre-heated SiC powder was gradually added into molten aluminium. Over the surface of molten Aluminium, nitrogen gas was supplied at a flow rate of 4 L/min and 1% of Magnesium was added and mechanically stirred. The mechanical stirrer is made of mild steel with AC power supply and its rotated at constant speed of 300 rpm. Then the temperature was maintained between 710 and 730 °C. Within next 15 min all the SiC powder were completely dropped in to the melt and for an additional duration of 10 min the stirring process was continued. After 25 min of stirring totally, the melt which was at 720 °C was poured in to the permanent mould and kept in atmospheric temperature to get solidified. Before pouring, the permanent mould was also preheated at 250 °C for 1 h so as to remove the moisture sticking with the mould.

Fabrication of in-situ formed Al/TiB_2 MMCs involves The Potassium Hexa Fluro Titanate (K_2TiF_6), Potassium Tetra Fluro Borate (KBF_4) and wrought Aluminium 6061 as the initiating materials. These halide salts with stoichiometric composition corresponding to 4 wt%, 6 wt% and 8 wt% of TiB_2 in the Al/TiB_2 composites were mixed. Melting of the aluminium was carried out in a graphite crucible. An electrical resistance furnace operating under normal ambient conditions was employed. The (K_2TiF_6) and (KBF_4) salts were preheated at 250 °C for 30 min before it was manually mixed into the molten aluminium that had been maintained at 820 °C followed by the 30 min stirring time. Heating was maintained at this temperature for 15 min to allow the in-situ TiB_2 particles to develop in the matrix. Nitrogen gas supplied through a fine copper tube was used at intervals to avoid atmospheric contamination. The dross was skimmed off twice from the surface of the melt, once before adding salts and the other just before the pouring. The composite melt was cast in a sand mould to produce a cast ingot as shown in Fig. 1.

Microstructural examination was carried out using light optical microscope (Make: MEJI, Japan; Model: MIL 7100) interfaced with image analysing software (Metal vision). The specimens were cut from the composites with as-cast and heat-treated conditions. All the sides of the samples were polished to ensure the flatness of the sample. The specimens for metallographic examination were roughly polished by the emery sheets with large grit size and subsequently polished using different grades of water emery papers to get fine polish. Final polishing was done using alumina powder in the disc polishing machine. The specimens were etched as per the ASTM standard E407 (Standard practice for micro etching of metals and alloys) with standard Keller's reagent made of 190 ml of distilled water, 5 ml of HNO_3, 3 ml of HCl and 3 ml of HF. The chemical etchants were swabbed and washed thoroughly in running water. After etching, the specimens were placed in the optical microscope to reveal the macrograph. Scanning Electron Microscopy (SEM) equipped with Energy-dispersive X-ray spectroscopy (EDX) analysis is mainly useful in understanding the main microstructure, fracture analysis, boundary studies and elements in the composites. To identify the phases, present in the fabricated MMCs, XRD and Element Mapping analysis were carried out.

3 Justification for Selection of Moulds

Sand mould has been selected for Al/TiB_2 MMC and permanent mould has been selected for Al/SiC MMC as castings made from both of these cases have uniform distribution of reinforcement particles throughout the casting and comparison could be more sensible as both Al/TiB_2 MMC and Al/SiC casts in the respective moulds have similarity of distribution of reinforcements.

Fig. 1 Cast ingot taken from mould

Table 1 Chemical composition of base metal (Al6061)

Elements	Mg	Si	Mn	Fe	Cu	Zn	Ti	Cr	Al
Composition (weight %)	0.85	0.69	0.067	0.214	0.221	0.013	0.025	0.077	Remaining

3.1 Al/TiB_2 MMC Cast in Sand Mould

The Al/TiB_2 MMC cast in sand mould has uniform distribution of reinforcement particles as the liquid metal in sand mould remains liquid for longer duration and circulations of liquid metal will not be set up because the liquid metal temperature throughout the mould will be almost equal resulting in no density differences of liquid metal in the sand mould until it solidifies finally.

3.2 Al/SiC MMC Cast in Permanent Mould

Though Al/SiC MMC is cast in permanent mould circulations of liquid metal may not be set up as the degree of superheat is much less as compared to that with Al/TiB_2 MMC and the Al/SiC MMC is expected to solidify within a very short time. Whereas, Al/TiB_2 MMC, if it is cast in permanent mould, circulations will be set up due to density differences at various locations of the permanent mould resulting due to temperature variations arising out of differing cooling rates prevailing from location to location of the permanent mould. If circulations are set up TiB_2 particle distribution are expected to be more in the locations where cooling rate is high and less in the locations where cooling rates are low [11–13].

If Al/SiC MMC is cast in sand mould then the liquid metal will remain liquid for longer duration due to the insulation provided by the sand and this might result in the bigger SiC particle of average size 22 µm, as used in this case, has every chance of settling down before solidification. Hence in this case of Al/SiC MMC, the casting, as it freezes without liquid metal circulations in the mould, is also expected to have uniform distribution of SiC particles [13].

4 Effect of SiC Particles Addition on Microstructure of Al/SiC MMCs (Ex-situ)

Figure 2a–d show the base metal and Al/SiC composite optical microstructures with varying weight percentage of SiC particles addition like 4 wt%, 6 wt% and 8 wt%. They display homogeneously dispersed SiC particles in the aluminium matrix, however some regional fine SiC particulate clusters appear in the Al/8 wt% SiC composite microstructure. Moreover, the particles act as nucleation sites and thus reduce the grain size considerably with increasing weight fraction of SiC particles in the matrix (Devi et al. 2013 and Knt et al. 2017). When 4 wt% and 6 wt% SiC particles are added to the aluminium melt (Fig. 2a, b), the particles are uniformly dispersed without any clustering in the matrix, while the 8 wt% SiC addition of particles causes the clustering of particles coupled with some fine pores (Fig. 2c).

Figure 3 show the SEM micrographs of base metal and synthesized Al/SiC composites. All the synthesized composites show the uniformly distributed SiC particles along with some regional clusters. The micrograph clearly reveals the maximum presence of SiC particles in the Al/8 wt% SiC composite, whereas, minimum number of particles were observed in the Al/4 wt% SiC composite. In addition, increasing the addition of SiC particles into the matrix, leads to the formation of agglomeration coupled with fine pin holes as shown in Fig. 3b–d.

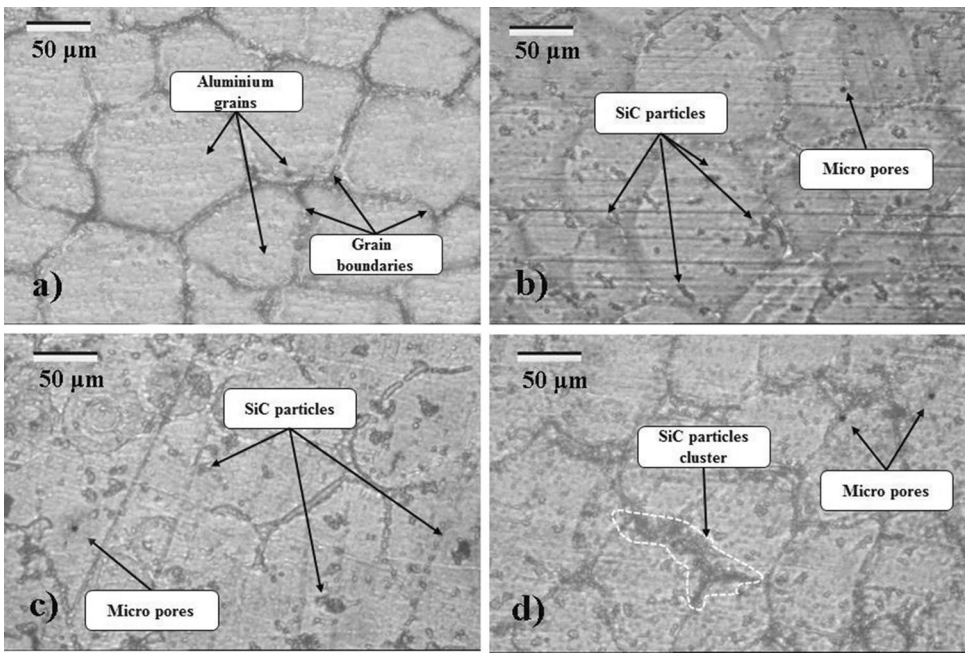

Fig. 2 Optical Microstructure of as-cast base metal and Al/SiC MMCs. **a** base metal, **b** Al/4 wt% SiC MMC, **c** Al/6 wt% SiC MMC and **d** Al/8 wt% SiC MMC

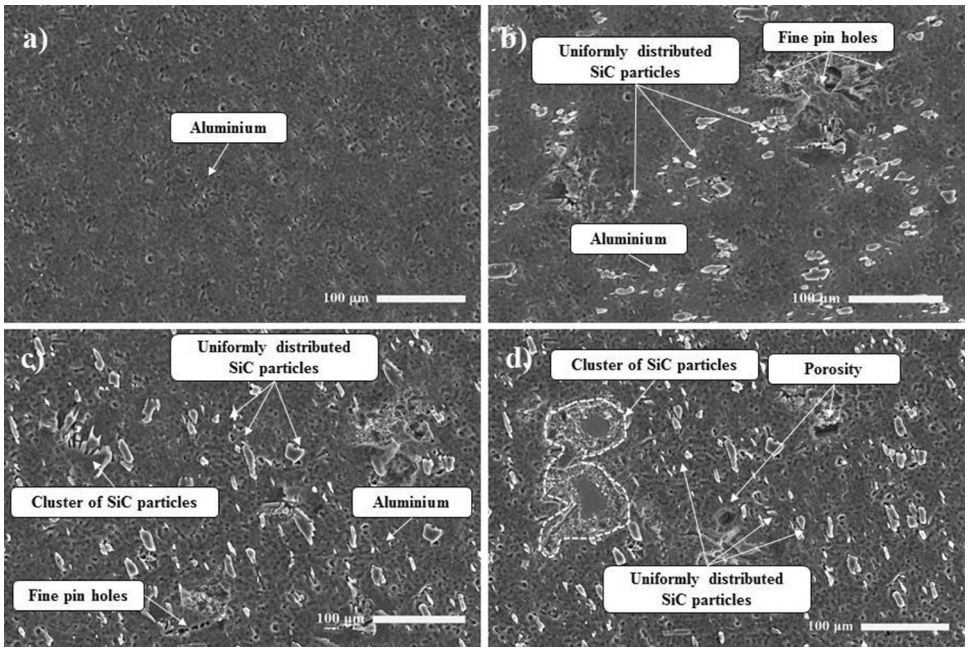

Fig. 3 SEM Micrographs of as-cast base metal & Al/SiC MMCs. **a** Base metal, **b** Al/4 wt% SiC MMC, **c** Al/6 wt% SiC MMC and **d** Al/8 wt% SiC MMC

The XRD patterns of base metal and ex-situ formed Al/SiC composites are shown in Fig. 4a–d. The XRD intensity exhibited that the composite materials consist of two main phases such as Al, SiC along with major alloying elements. As it is seen, SiC intensity increases with increase in weight fraction SiC particles and similar trend can be observed in the optical and SEM micrographs. EDS spot analysis (Fig. 5) confirms the grey colour spots indicating Si and C element and dark black colour spot designate the Al alloys which confirms the presence of SiC particles in Al matrix. Figure 6 shows the results of element mapping analysis of Al/8 wt% SiC composite. As it is seen, there are many different colour phases (Si-4.2%, Mg-1.2%, C- 4.6%, Fe-0.21%, Cu-0.2% and Al-89.59%) which confirms the existence of SiC reinforcement in the aluminium matrix coupled with alloying elements e.g., Si, Mg, Fe and Cu in the composite.

4.1 Effect of SiC Particles Addition on Macro Hardness of Al/SiC MMCs

Table 2 shows mechanical properties of synthesized Al/SiC MMCs. Noteworthy increase in the hardness can be found with increase in weight percentages of SiC content [3] (Rahmani Fard et al. 2007). The maximum increment of hardness obtained in the Al/8 wt% of SiC composite over base metal is 25% and the minimal increment of hardness is 3.84% in the Al/4 wt% of SiC composite over base metal. Whenever, the hard-reinforcing phases were fused into a soft ductile matrix, the hardness of the composite is improved. Generally, When the SiC particle, which is a hard-ceramic phase (properties superior than base alloy) is incorporated into soft aluminium matrix it resists the dislocation movement and hence, the hardness of the composite improves [5].

4.2 Effect of SiC Particles Addition on Tensile Property of Al/SiC MMCs

Figure 7 shows Engineering stress strain curves of as-cast Al/SiC MMCs. Values of 0.2% proof strength, ultimate tensile strength and percentage elongation of synthesized Al/SiC composites are shown in Table 2 and it is obvious that all the synthesized composites have higher 0.2% proof strength and ultimate tensile strength as compared to base matrix alloy [6, 8]. Maximum enhancements of 0.2% proof strength and ultimate tensile strength are 65.78% and 44.76% respectively for Al/8 wt% of SiC composite and minimum enhancements of 28.94% and 20% for Al/4 wt% of SiC composite were observed as compared to base as-cast alloy.

It is due to the fact that, increase in weight fraction of SiC particles in the aluminium matrix result in better tensile strength, yield strength and hardness, but the percentage of elongation of the composite is decreased significantly. The percentage elongation of base metal is 20.2% and that of Al/8 wt% of SiC composite is 13.8%. Generally, the tensile property is a function of the nature and properties of matrix and reinforcement materials. The compatibility of the matrix and reinforcement also play a dominate role for achieving the better UTS of the composites. The reinforcing particles act as barrier to the movement of dislocation under load. Thereby, more loads are required for nucleation of voids and their propagation, leading to higher tensile strength in the composites [8]. The UTS of the composite enhances with

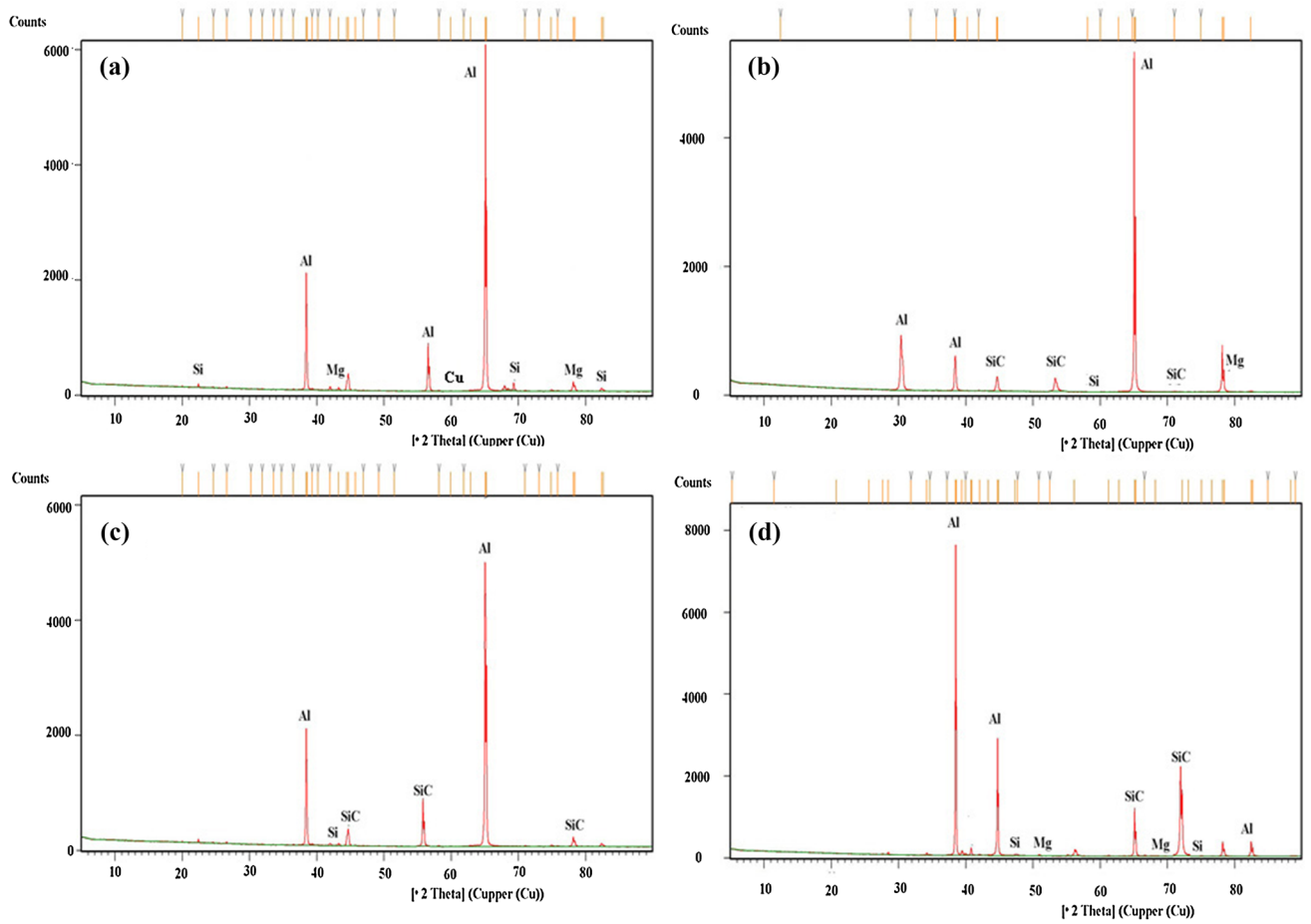

Fig. 4 XRD results of as-cast base metal and Al/SiC MMCs. **a** Base metal, **b** Al/4 wt% SiC MMC, **c** Al/6 wt% SiC MMC and **d** Al/8 wt% SiC MMC

increase in the weight percentage of SiC particles present in the composites.

4.3 Fractography of Al/8 wt% SiC Composite

Figure 8 shows the fracture morphology of as-cast base metal and Al/8 wt%SiC composites. As shown in Fig. 8a, many large dimples are existing on the fracture surface. Meantime, the tearing edges include smaller dimples. It is demonstrated that of great plastic deformation occurs just before fracture. Hence, the fracture of base metal was inferred to be ductile and could have happened by the development and combination of micro-voids. Besides, during tensile testing, the development of micro-void is originated under the local three-dimensional state of stress and increase with increasing the tensile load [9]. Finally, the voids reach to a critical size and failure happened due to merging of such micro-voids. Figure 8b shows fractured surfaces of the fabricated Al/8 wt%SiC composites. The fractography of specimen shows few shallow dimples along with massive number of fairly flat and smooth zones, named as mirror regions. The existence of mirror regions is the cause of sudden break of the matrix which is indicating a very low plastic deformation before failure. This type of fracture is more stable in materials with relatively low ductility [9].

5 Effect of TiB_2 Particles Addition on Microstructure of Al/TiB_2 MMCs (In-situ)

Figures 9 and 10 show the optical and SEM micrographs of base metal and fabricated composites. All synthesized composites confirm the presences of TiB_2 particles along with flake like Al_3Ti intermetallic [11] The size and uniformity of TiB_2 particles is confirmed by SEM micrographs (Fig. 10) and the average size of the particles lies between 0.5 µm to 2 µm [12]. The micrographs show obviously the maximum TiB_2 formation in 8 wt% TiB_2 composite and minimum in 4 wt% TiB_2 composite. Moreover, the formation of Al_3Ti

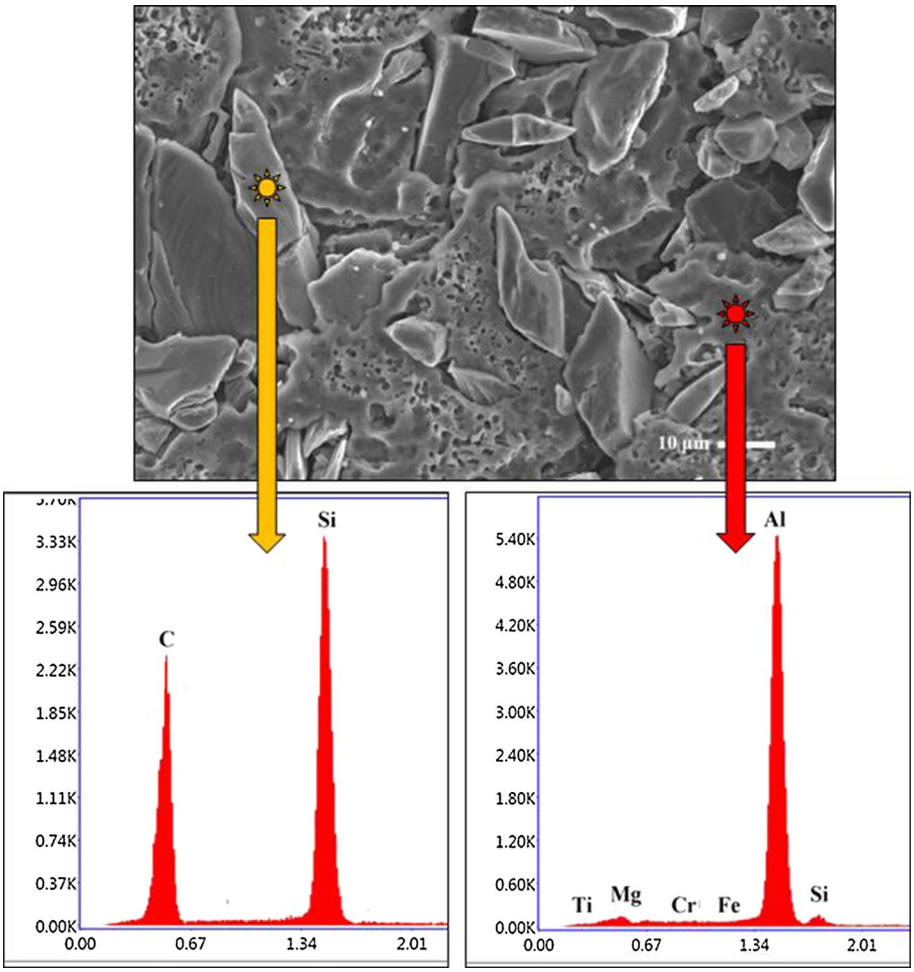

Fig. 5 EDX spot analysis of as-cast Al/8 wt% SiC MMC

intermetallic increase with increasing the weight fraction of TiB_2 reinforcement addition into the matrix materials [14–20].

In these optical micrographs, TiB_2 particles appear as black particles surrounded by aluminium matrix (yellow colour) whereas in SEM micrographs the TiB_2 particles look white in colour and surrounded by aluminium matrix appearing black in colour.

The reinforcement and matrix interfaces are almost free of porosity due to the enhancement of wettability by in-situ reaction taking place between the precursor salts. Moreover, Fig. 9b–d reveals, some regional clusters of TiB_2 particles and located in grain boundaries. During solidification process, the fine TiB_2 particles are pushed away by the solidification front towards the interdendritic region [13, 14].

Besides, numerous numbers of elongated dendritic grains appear in the composite as shown in Fig. 9b–d. When the formation of TiB_2 particles in the composite increases, the grains slowly become equiaxed. Figure 9d shows the reduction of average grain size with increasing number of TiB_2 particles. The mechanism and formation of in-situ TiB_2 particles are explained by the following sections.

5.1 Mechanism of In-situ formed TiB_2 particles

Exothermic reaction mechanisms start with the stoichiometric ratio 1:2 of two types of halide salts. It can be seen that TiB_2 cannot be directly formed from the reduction of K_2TiF_6 and KBF_4. First, K_2TiF_6 and KBF_4 in the Al melt decompose in to KF liquid, titanium fluoride and boron fluoride gases. Then Ti and B ions are released, that diffuse into liquid Al and by aluminothermic reduction form titanium fluoride and boron fluoride gases at the molten flux-liquid metal interface. Where, by products KF, F, AlF_3 are not useful and were removed as slag or natural volatilization (a substance that is easily evaporated at normal temperature) prior to casting. In the second step of the reaction, the solutes Ti and B in liquid Al reach saturation and they will be separated out as the intermetallic compounds TiB_2, Al_3Ti and AlB_2 according to equations [20–24].

$$Al + K_2TiF_6 \rightarrow 2KF + TiF_4 + Al \quad (5.1)$$

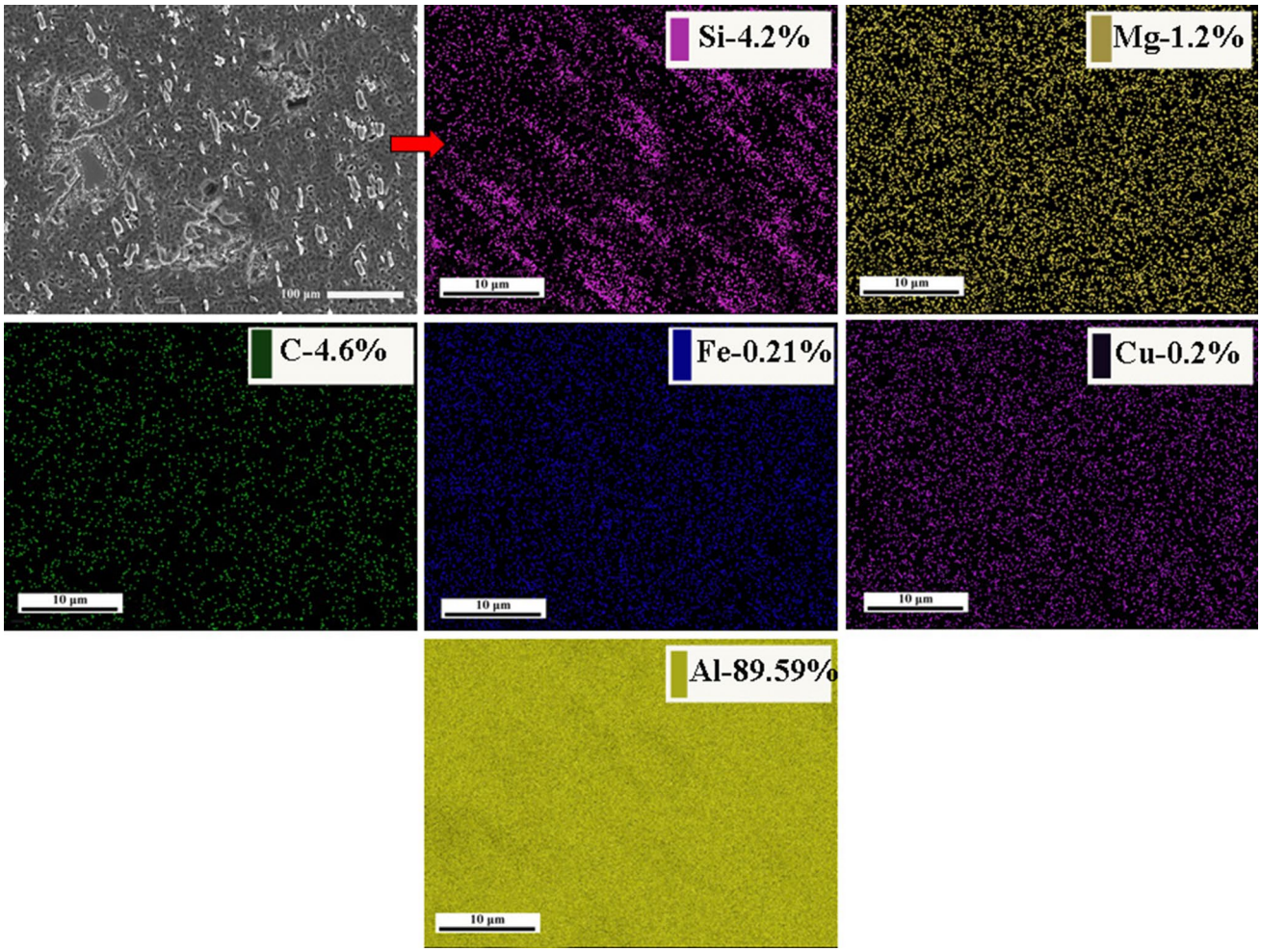

Fig. 6 Element mapping of as-cast Al/8 wt% SiC MMC

Table 2 Mechanical properties of Al/SiC MMCs as-cast condition

s.no	Synthesized materials	As-cast condition			
		Rockwell hardness (R_B)	0.2% proof strength (MPa)	Ultimate tensile strength (MPa)	Elongation in gauge length (%)
1	Base metal	52	76	105	20.2
2	Al/4 wt% SiC	54	98	126	17.8
3	Al/6 wt% SiC	60	116	134	19.4
4	Al/8 wt% SiC	65	126	152	13.8

$$Al + 2KBF_4 \rightarrow 2KF + 2BF_2 + Al \quad (5.2)$$

$$Ti + 2B \rightarrow TiB_2 \quad (5.4)$$

$$2KF + TiF_4 + Al + 2KF + 2BF_3 + Al \rightarrow 4KF + 2AlF_3 + 2F_2 + Ti + 2B \quad (5.3)$$

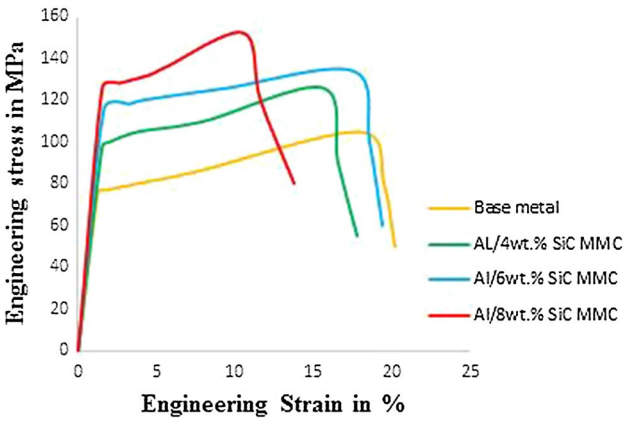

Fig. 7 Engineering stress strain curves of as-cast base metal & Al/SiC MMCs

Often by product were formed small amount i.e.,

$$Ti + 3Al \rightarrow Al_3Ti \tag{5.5}$$

$$2B + Al \rightarrow AlB_2. \tag{5.6}$$

5.2 Formation of TiB_2 Particles by In-situ Technique

The stoichiometric proportions of K_2TiF_6 and KBF_4 salts were mixed and preheated to 250 ˚C and soaked for 30 min. The mixed and preheated salts of Potassium Hexa Fluro Titanate and Potassium Tetra Fluro Borate are introduced into an aluminium melt. The preheated salts react in presence of liquid aluminium, forming TiB_2 precipitates within aluminium as shown in Fig. 11a. The reactions take place until TiB_2 is formed. The volatile by product fluron gas escapes from the melt as gas as shown in Fig. 11b.

The other by products AlF_3 and KF were removed as slag. When the Titanium bearing (K_2TiF_6 salt) and Boron bearing (KBF_4 salt) powder particles come in contact during mixing in aluminium melt the reaction might begin releasing fluron gas. At the same time due to the exothermic reaction occurring locally between the halide salts powder particles the temperature will shoot up enormously forming TiB_2 molecules. Between the TiB_2 molecules the fluron gas formed as a by-product will try to escape out, causing low pressure between the TiB_2 molecules, than the surroundings. The surrounding aluminium liquid will eventually consolidate the TiB_2 molecules together and a bigger TiB_2 particle will result. Slowly with time the surrounding TiB_2 molecules formed will attach themselves to the TiB_2 particle already formed and growth in size may thus take place. This growth in size will cease when the reaction is complete. The formation of in-situ formed TiB_2 particle in the aluminium melt was summarized elsewhere [15, 17] The intermetallic phases such as Al_3Ti and AlB_2 are predominantly observed in the composite synthesized via in-situ reaction. The occurrence of this intermetallic was justified due to the unstable nature of Al_3Ti and AlB_2 in a reaction mixture comprising Ti/B ratio greater than 1/2. Even though, after attaining a certain limit, Al_3Ti formed is stable in the aluminium melt due to deficiency of boron atoms. Auradi et al. 2014 has studied Microstructure and Mechanical Characterization of Al-TiB_2 In-situ metal matrix composites produced via master alloy route and reveal the presence of white, hexagonal TiB_2 particles with fairly uniform distribution in a-Al matrix along with traces of Al_3Ti particles through SEM analysis. Ramesh et al. [8] has studied microstructural and mechanical properties of Al 6061/TiB_2 in-situ composites. The optical microphotographs of Al 6061 alloy and the developed composites show the uniformly distributed TiB_2 particles along with traces of flake like Al_3Ti.

Figure 12a–d illustrate the XRD result of Al/TiB_2 MMCs and it is evident that the higher intensity of peaks were Al

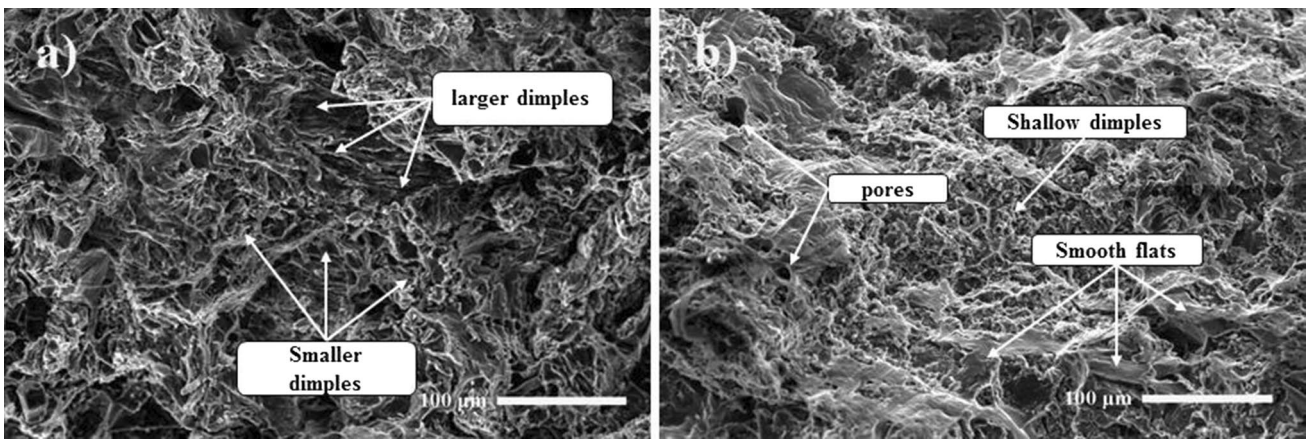

Fig. 8 Fractography of **a** as-cast base metal and **b** Al/8 wt% SiC MMC

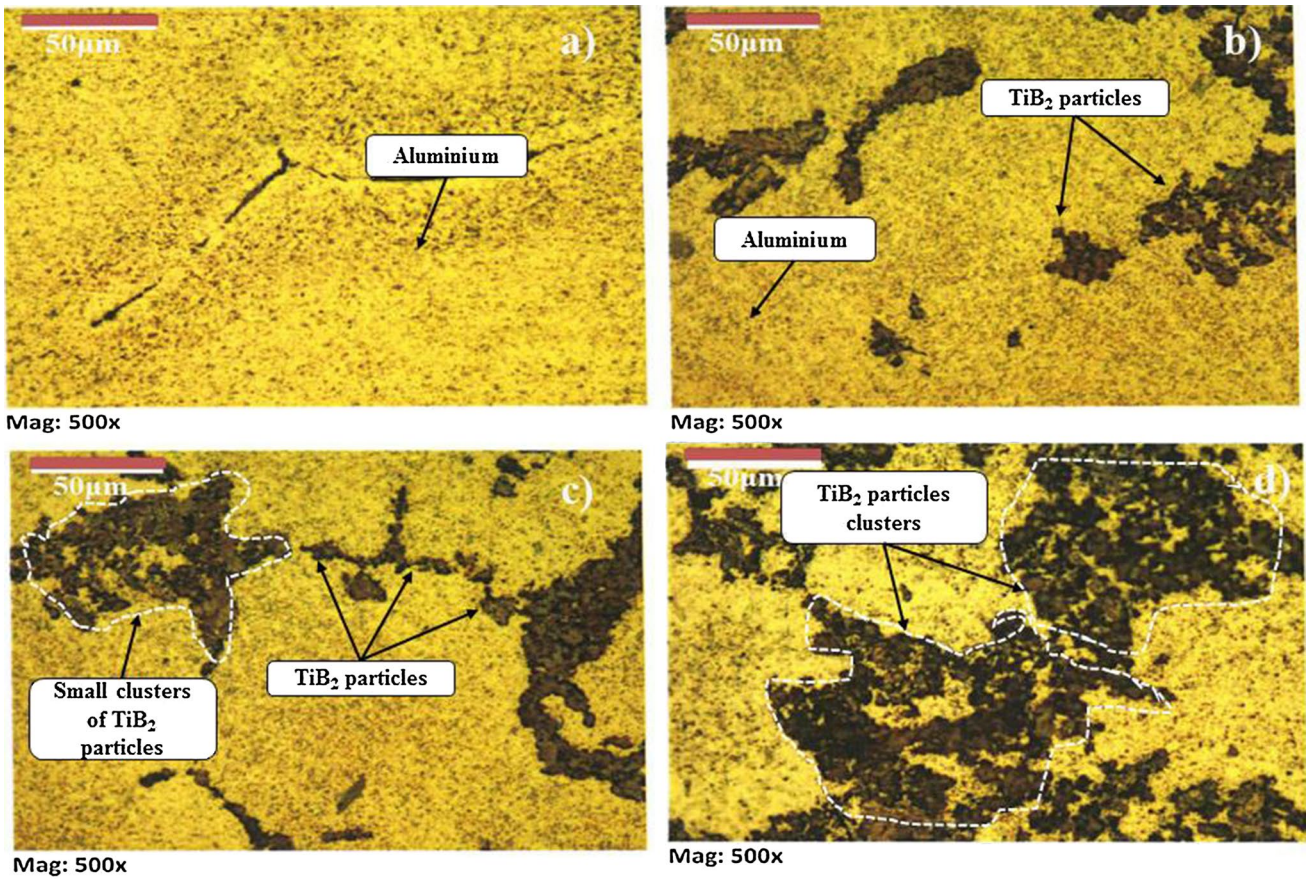

Fig. 9 Optical microstructure of as-cast base metal & Al/TiB_2 MMCs. **a** base metal, **b** Al/4 wt% TiB_2 MMC, **c** Al/6 wt% TiB_2 MMC and **d** Al/8 wt% TiB_2 MMC

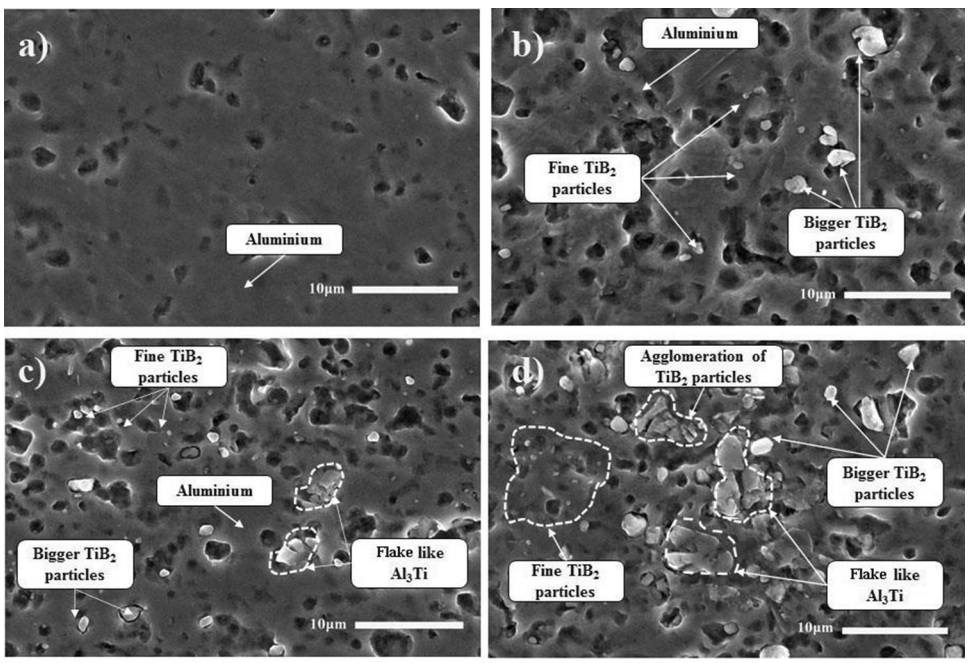

Fig. 10 SEM micrograph of as-cast base metal & Al/TiB_2 composites. **a** Base metal, **b** Al/4 wt% TiB_2 MMC, **c** Al/6 wt% TiB_2 MMC and **d** Al/8 wt% TiB_2 MMC

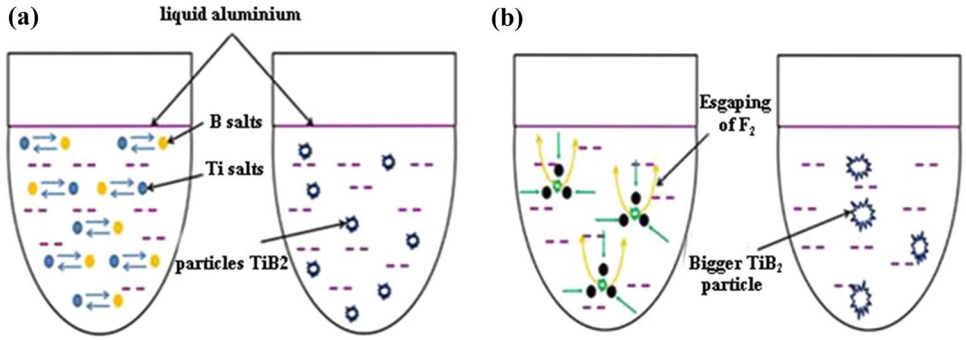

Fig. 11 Formation of in-situ formed TiB_2 particles (**a**) Formation of TiB_2 particles and (**b**) Escape of F_2 gas

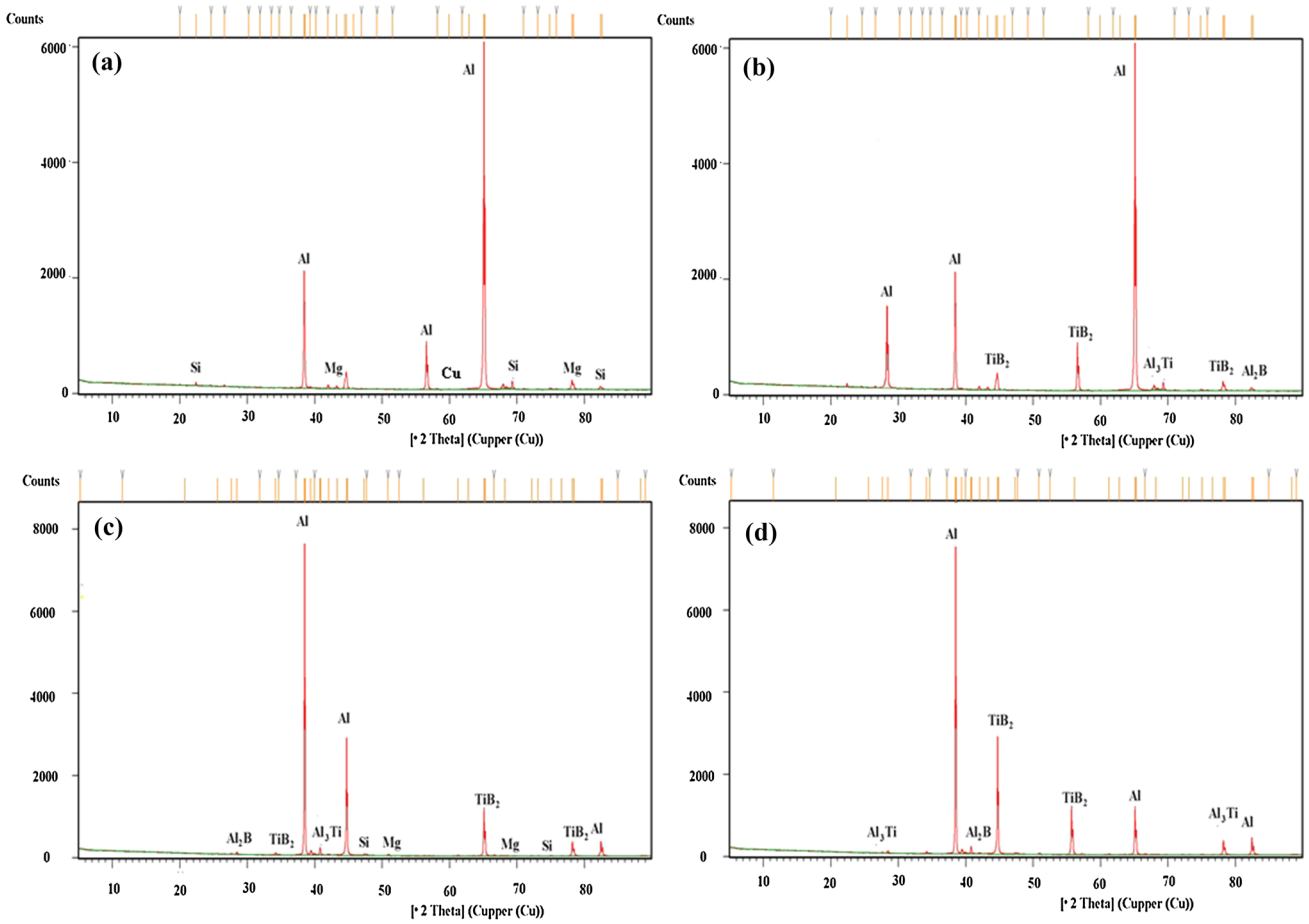

Fig. 12 XRD results of as-cast base metal & Al/TiB_2 MMCs. **a** Base metal, **b** Al/4 wt% TiB_2 MMC, **c** Al/6 wt% TiB_2 MMC and **d** Al/8 wt% TiB_2 MMC

and TiB_2, confirming the presence of TiB_2 reinforcement, are distributed in the aluminium matrix. Moreover, the intermetallics such as Al_3Ti and AlB_2 were observed. As mentioned earlier the Al_3Ti intensity of peak increased with increasing the addition of TiB_2 particles in the aluminium matrix [18].

EDS spot analysis (Fig. 13) confirmed that the white colour spots that indicate Ti and B element and dark black colour spot designate the Al alloys. Figure 14 shows the results of element mapping analysis of Al/8 wt% TiB_2 composite. As it is seen, there are many different colour phases (Si-1.62%, Mg-1.27%, B-6.02%, Ti-4.52%, Fe-0.19% and Al-86.38%) which confirm the existence of TiB_2 reinforcement in the aluminium matrix coupled with intermetallics e.g., Al_3Ti and AlB_2 in the composite. Moreover, the major

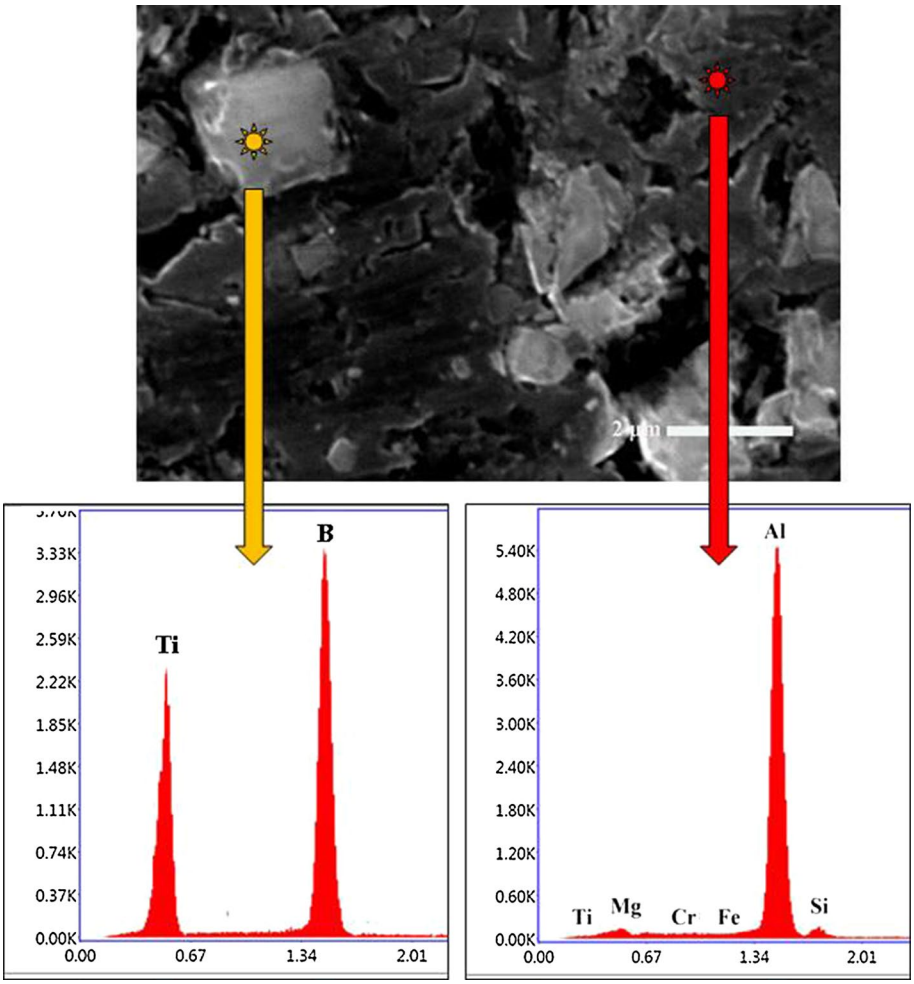

Fig. 13 EDX spot analysis of as-cast Al/8 wt% TiB_2 MMC

and minor allying elements are once again conformed by the element mapping analysis.

5.3 Effect of TiB_2 Particles Addition on Macro Hardness of Al/TiB_2 MMCs

Table 3 shows results obtained from Rockwell hardness testing of base metal and its in-situ formed TiB_2 composites. As it is seen, substantial enhancements in the hardness was observed with the addition of TiB_2 particles in the aluminium matrix. A maximum enhancement of 34.61% and a minimum enhancement of 15.38% are observed for Al/8 wt% of TiB_2 composite and Al/4 wt% of TiB_2 composite respectively. TiB_2 is a hard-ceramic reinforcement, it is incorporated into soft aluminium matrix that result in the increased resistance to deformation and hence hardness of the composite material was enhanced [12]. The grain refinement and fineness of the reinforcement also play a significant role for deciding the hardness of the composite materials. As the exothermic reaction takes place during in-situ composite fabrication, the fine and clear interfacial bonding is achieved. In other words, the production technique and soundness of the casting significantly improve the hardness of composite [20]. Reaction free interface promote the load transfer capability from matrix to reinforcement.

The hardness of the composite increases with increasing load transfer capability of matrix to the reinforcement. It is concluded that uniformity of TiB_2 particles coupled with reaction free interface between matrix and reinforcement enable efficient transfer of load from matrix to reinforcement. Thus, improvement of hardness of the synthesized composites take place [25].

5.4 Effect of TiB_2 particles addition on tensile property of Al/TiB_2 MMCs

Figure 15 shows the Engineering stress strain curves for as-cast Al/TiB_2 MMCs and Table 3 shows the variation of 0.2% proof strength, ultimate tensile strength and percentage of elongation of fabricated in-situ formed composites as a function of the weight fraction of TiB_2 particles. It is evident that, the 0.2% proof strength and ultimate tensile strength of all synthesized composites are higher than base aluminium matrix and their magnitudes increase with the

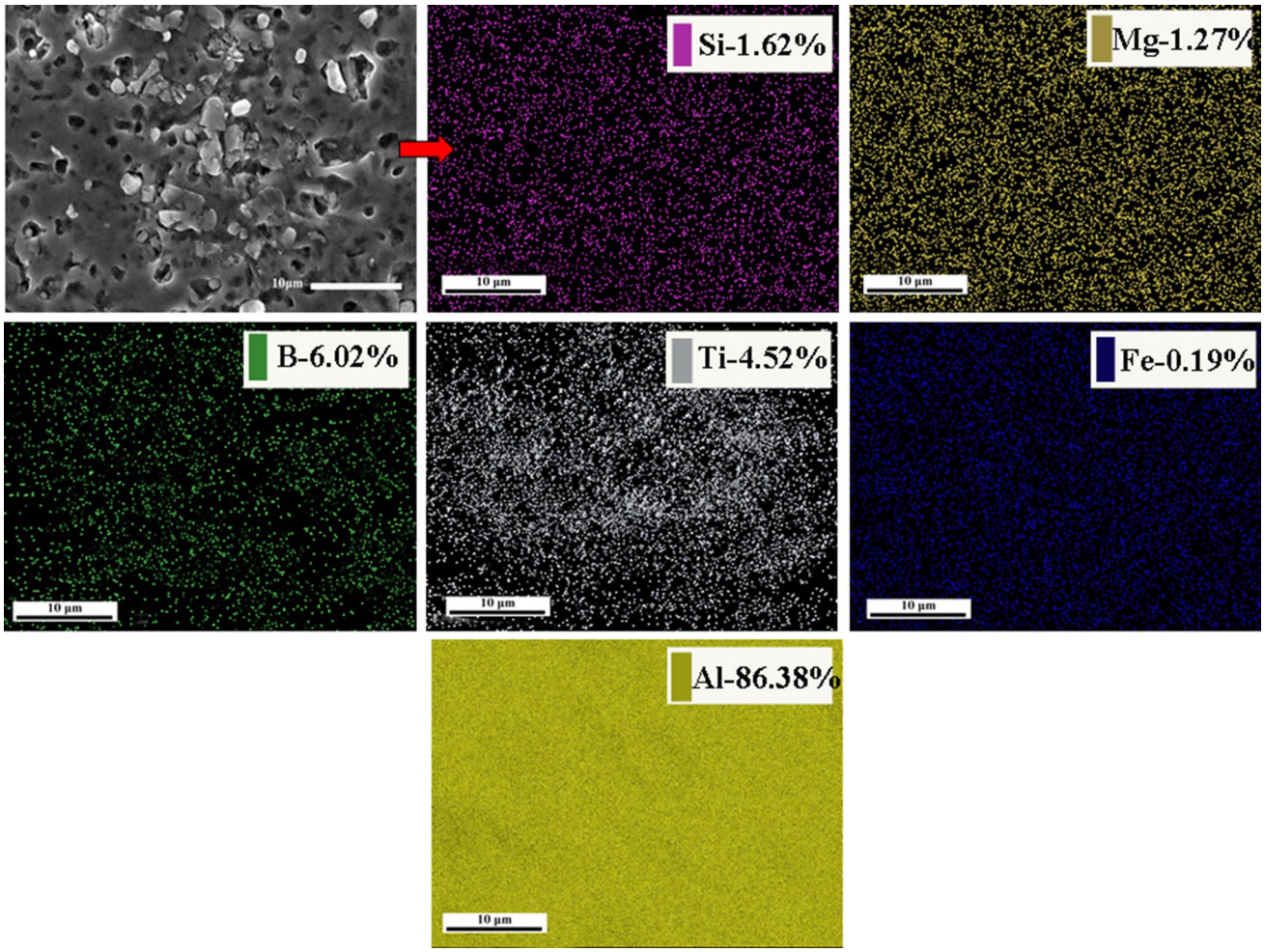

Fig. 14 Element mapping analysis of as-cast Al/8 wt% TiB_2 MMC

Table 3 Mechanical properties of Al/TiB_2 MMCs as-cast condition

s.no	Synthesized materials	As-cast condition			
		Rockwell hardness (R_B)	0.2% Proof strength (σ_y) in MPa	Ultimate tensile strength (σ_u) in MPa	Elongation in gauge length (%)
1	Base metal	52	76	105	20.2
2	Al/4 wt% TiB_2	60	102	133	19.4
3	Al/6 wt% TiB_2	67	128	146	17.4
4	Al/8 wt% TiB_2	70	136	170	12.8

increase in weight fraction of TiB_2 particles with significant loss of elongation [14]. Moreover, 0.2% proof strength and ultimate tensile strength of Al-8 wt% TiB_2 are 136 MPa and 170 MPa respectively which are 78.94% and 61.90% higher than base aluminium matrix. 0.2% proof strength and ultimate tensile strength of Al-4 wt% TiB_2 are 102 MPa and 133 MPa respectively which are 34.21% and 26.67% higher than base aluminium matrix.

The percentage elongation of base metal is 20.2% and that of Al/8 wt% of SiC composite is 12.8%. Effect of TiB_2 particles addition on strength of aluminium based composites can be arrived by two diverse approaches. One is based on the effective load transfer capability from matrix to reinforcement in which the bonding strength and quality of casting has been paid an extensive role and the second is based on the influence of TiB_2 particles on yield strength of aluminium matrix [21].

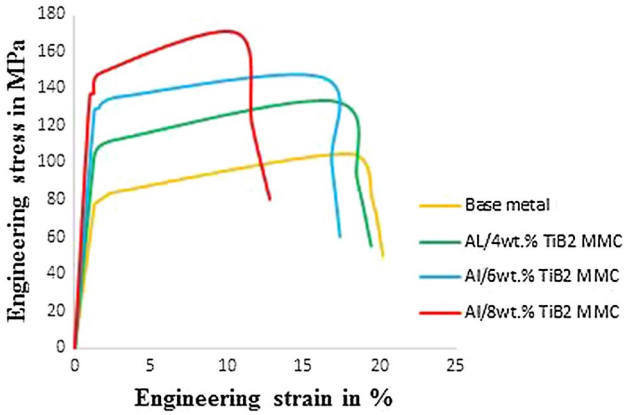

Fig. 15 Engineering stress strain curves of as-cast base metal & Al/TiB_2 MMCs

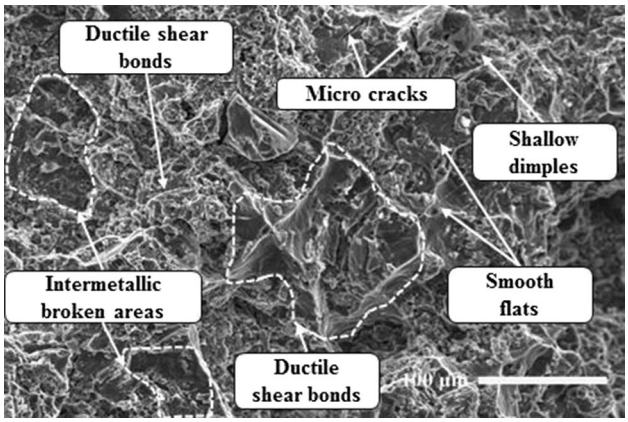

Fig. 16 Fracture surface of as-cast Al/8 wt% TiB_2 MMC

According to the first approach, the yield strength of composite can be described as a function of the volume fraction of reinforcement through the following expression [23] ,

$$\sigma_{yc} = \sigma_{ym}[v_p(1 + s/2) + (1 - v_p)] \quad (5.7)$$

where v_p—the volume fraction of reinforcement, s—the aspect ratio of particles, σ_{ym}—the yield strength of matrix and σ_{yc}—the yield strength of composite. It is observed that, increasing the quantity of TiB_2 content improves the load bearing capacity, so as yield strength of the composite was enhanced [24]. Second approach includes three different mechanisms: first mechanism is the grain refinement of matrix i.e., by incorporating TiB_2 particles into matrix phase (Hall-Petch effect). It is realized that the grain boundaries act as impediments for dislocation movement and hence lead to the improvement of yield stress. TiB_2 particles inhibit grain growth of aluminium matrix phase and increase the area fraction of grain boundaries. Second mechanism is the Orowan strengthening effect of TiB_2 particles. As stated by this mechanism, high volume fraction of fine and sub-micron size of TiB_2 particles, dispersed uniformly in the aluminium matrix, would be to act as impediments for dislocation movement [12]. Hence, dislocation loops are induced around TiB_2 particles, that increase the stress necessary for further deformation. Third is the formation of residual plastic strain in between the matrix and reinforcement due to the thermal mismatch of co-efficient of thermal expansions resulting in the raise in dislocation density [25–30]. Thus, the above discussed phenomena are applicable for the Al/TiB_2 composite regarding the increase in strength.

5.5 Fractography of Al/8 wt% TiB_2 composite

Figure 16 illustrate the fracture surface of the Al/8 wt% TiB_2 composite. It reveals the coexistence of ductile and brittle fractures. The presence of fine shasllow dimples along with the ductile shear bands demonstrate the ability of ductile retainment by the composite. In addition, the existence of smooth flats and microcracks indicate the brittle fracture and these are observed away from the dimples and shear bands and thus brittle fracture was initiated by the Al_3Ti intermetallics [23].

6 Conclusion

The effect of reinforcement particles addition on microstructure and mechanical properties were analysed and the following important finding were observed.

- Increase in reinforcement particles to the base alloy tends to increase the presence of SiC and TiB_2 particles with some reginal clusters and intermetallic phases. Increasing in weight fraction of reinforcement particles make the grains slowly become equiaxed. The reduction of average grain size was noticed with increase in the number of TiB_2 particles.
- For Al/8 wt% of SiC composite, the maximum enhancement of 0.2% proof strength, ultimate tensile strength and hardness are 65.78% and 44.76% and 25% respectively over base metal. Whereas, 78.94% and 61.90% and 34.61% improvements were noticed when composite synthesized with Al/8 wt% of TiB_2 addition as compared to base as-cast alloy.
- It is concluded that Al/TiB_2 MMCs have better mechanical properties as compared to Al/SiC MMCs as well as base metal. It is because, the exothermic reaction takes place between the matrix and the precursor salts. Hence, the severe agitation is induced within the molten metal. Because of this agitation, TiB_2 particles are uniformly segregated throughout the entire matrix materials.

Acknowledgements The authors would like to acknowledge the Department of Manufacturing Engineering, Annamalai University and University Grant Commission (UGC)-RGNF, New Delhi, India for supporting this research work.

References

1. C.N. Devi, N. Selvaraj, V. Mahesh, Micro structural aspects of aluminium silicon carbide metal matrix composite. Int. J. Appl. Sci. Eng. Res. **1**(2), 250–254 (2013)
2. S. Mozammil et al., A review on hot extrusion of Metal Matrix Composites (MMC's). Mater. Sci. Eng. A, 620–648 (2015)
3. S. Kayal, R. Behera, G. Sutradhar, Mechanical properties of the as-cast silicon carbide particulate reinforced Aluminium alloy Metal Matrix Composites. Int. J. Curr. Eng. Sci. Res. **2**(3), 318–322 (2012)
4. S. Kant, A. Singh Verma, Stir casting process in particulate aluminium metal matrix composite: a review. Int. J. Mech. Solids **9**(1), 973–1881 (2017)
5. N. Parvin, R. Assadifard, P. Safarzadeh, S. Sheibani, P. Marashi, Preparation and mechanical properties of SiC-reinforced Al6061 composite by mechanical alloying. Mater. Sci. Eng. A **492**(1–2) 134–140 (2008)
6. G.J. Naveen, Microstructure and mechanical properties comparison of Cast and Extruded Al6061-SiCp composites. IJRITCC **2**(10), 2982–2984 (2014)
7. R.K. Goswami, R. Sikand, A. Dhar, O.P. Grover, U.C. Jindal, A.K. Gupta, Extrusion characteristics of aluminium alloy/SiC p metal matrix composites. Mater. Sci. Technol. **15**(4), 443–449 (1999)
8. C. Ramesh, A. Hirianiah, K. Harishanad, N.P. Noronha, A review on hot extrusion of Metal Matrix Composites (MMC's). Int. J. Eng. Sci. **1**(10), 30–35 (2012)
9. A. Bahrami, A. Razaghian, M. Emamy, R. Khorshidi, The effect of Zr on the microstructure and tensile properties of hot-extruded Al-Mg_2Si composite. Mater. Des. **36**, 323–330 (2012)
10. A. Bahrami, A. Razaghian, M. Emamy, H.R. Jafari Nodooshan, G.S. Mousavi, Microstructure and tensile properties of Al-15 wt%Mg_2Si composite after hot extrusion and heat treatment. Key Eng. Mater. **471–472**, 1171–1176 (2011)
11. B.S. Mandal, Murty, M. Chakraborty, Sliding wear behaviour of T6 treated A356-TiB_2 in-situ composites. Wear **266**(7–8), 865–872 (2009)
12. N. Kumar, G. Gautam, R. Kumar, G. Anita, M. Sunil, Synthesis and characterization of TiB_2 reinforced aluminium matrix composites: a review. J. Inst. Eng. Ser. D **97**(2), 233–253 (2016)
13. S. Lakshmi, L. Lu, M. Gupta, In situ preparation of TiB_2 reinforced Al based composites. J. Mater. Process. Technol. **73**(1–3), 160–166 (2002)
14. S. Suresh, N. Shenbaga Vinayaga Moorthi, S.C. Vettivel, N. Selvakumar, G.R. Jinu, Effect of graphite addition on mechanical behavior of Al6061/TiB_2 hybrid composite using acoustic emission. Mater. Sci. Eng. A **612**, 16–27 (2014)
15. C. Rajaravi, P.R. Lakshminarayanan, Experimental and FEA of fracture toughness on in-situ Al/TiB_2 MMCs in different mould conditions. IRJET **3**(1), 828–832 (2016)
16. C. Rajaravi, P.R. Lakshminarayanan, Effect of pouring temperature on A356-TiB_2 MMCs cast in sand and permanent moulds by in-situ method. JMBM **25**(5–6), 165–169 (2017)
17. P.S. Kumar, P.R. Lakshminarayanan, R. Varahamoorthi, Effect of pouring temperature on the TiB_2 in cast Al/TiB_2 MMC and prediction of distribution pattern by commercial simulation software. Adv. Nat. Appl. Sci. **11**(4), 321–331 (2017)
18. K. Niranjan, P.R. Lakshminarayanan, Optimization of process parameters for in situ casting of Al/TiB_2 composites through response surface methodology. Trans. Nonferrous Met. Soc. China **23**(5), 1269–1274 (2013)
19. S. Kumar, M. Chakraborty, V.Subramanya Sarma, B.S. Murty, Tensile and wear behaviour of in situ Al-7Si/TiB_2 particulate composites. Wear **265**(1–2), 134–142 (2008)
20. S.M. Mallikarjuna, U.S. Shashidhara, Mallik, K.I. Parashivamurthy, Grain refinement and wear properties evaluation of aluminum alloy 2014 matrix-TiB_2 in-situ composites. Mater. Des. **32**(6), 3554–3559 (2011)
21. K.L. Tee, L. Lu, M.O. Lai, In situ processing of Al-TiB_2 composite by the stir-casting technique. J. Mater. Process. Technol. **89–90**, 513–519 (1999)
22. B. Gobalakrishnan, P.R. Lakshminarayanan, R. Varahamoorthi, Combined effect of TiB_2 particle addition and heat treatment on mechanical properties of Al6061/TiB_2 in-situ formed MMCs. J. Adv. Microsc. Res. **12**(3), 230–235 (2017)
23. B. Gobalakrishnan, P.R. Lakshminarayanan, R. Varahamoorthi, Mechanical properties of Al 6061/TiB_2 in-situ formed metal matrix composites. J. Adv. Microsc. Res. **13**(1), 125–130 (2018)
24. B. Gobalakrishnan, P.R. Lakshminarayanan, R. Varahamoorthi, Effect of TiB_2 particle addition on the mechanical properties of Al/TiB_2 in situ formed metal matrix composites. Mater. Test. **60**(12), 1221–1224 (2018)
25. Y. Chen, D.D.L. Chung, In situ Al-TiB composite obtained by stir casting. J. Mater. Sci. **31**(2), 311–315 (1996)
26. S. Suresh, N.S.V. Moorthi, Aluminium-titanium diboride (Al-TiB_2) metal matrix composites: Challenges and opportunities. Procedia Eng. **38**, 89–97 (2012)
27. K.L. Tee, L. Lü, M.O. Lai, Improvement in mechanical properties of in-situ Al-TiB_2 composite by incorporation of carbon. Mater. Sci. Eng. A **339**(1–2), 227–231 (2003)
28. A. Mandal, M. Chakraborty, B.S. Murty, Ageing behaviour of A356 alloy reinforced with in-situ formed TiB_2 particles. Mater. Sci. Eng. A **489**(1–2), 220–226 (2008)
29. S. Johny James, K. Venkatesan, P. Kuppan, R. Ramanujam, Comparative study of composites reinforced with SiC and TiB_2. Procedia Engineer **97**, 1012–1017 (2014)
30. N. Ehsani, F. Abdi, H. Abdizadeh, H.R. Baharvandi, The effect of TiB_2 powder on microstructure and mechanical behavior of Al-TiB_2 metal matrix composites. Proc. SPIE **6423**, 642369 (2008)
31. V. Auradi, S.L. Biradar, S.M. Suresh, S.A. Kori, Microstructure and mechanical characterization of Al-TiB_2 In-situ metal matrix composites produced via master alloy route. Appl. Mech. Mater. **592–594**, 494–498 (2014)
32. C.S. Ramesh, S. Pramod, R. Keshavamurthy, A study on microstructure and mechanical properties of Al 6061 – TiB_2 in-situ composites. Mater. Sci. Eng. A **528**(12), 4125–4132 (2011)